SolarPACES 2022, 28th International Conference on Concentrating Solar Power and Chemical Energy Systems
Thermal Energy Storage Materials, Media, and Systems
https://doi.org/10.52825/solarpaces.v1i.727
© Authors. This work is licensed under a Creative Commons Attribution 4.0 International License
Published: 01 Mar. 2024

Cyclic Thermal and Structural Testing of a Hot Particle Storage Bin

Jeremy Sment[1][https://orcid.org/0000-0003-4700-7544], Kaden Plewe [2][https://orcid.org/0000-0002-8682-6879], Nathan Schroeder[1], Matthew Lambert[3], Dongmei Chen[2][https://orcid.org/0000-0002-3260-9385], and Clifford K. Ho[1][https://orcid.org/0000-0002-2994-9450]

[1] Sandia National Laboratories, USA

[2] University of Texas at Austin, USA

[3] Allied Mineral Products, LLC, USA

Abstract. Thermal energy storage is a key element in concentrating solar energy systems. In 2017 a Roadmap toward a third-generation system that could meet the SunSHOT goals of 0.06 $/kW$_e$ recommended increasing temperatures to > 700° C for heat transfer media to increase thermal efficiencies and lower levelized costs of heat. In 2021, the U.S. Department of Energy selected the particle pathway, G3P3, to build a 1 MW$_t$ prototype solar tower with 6 MWh thermal energy storage at the NSTTF in Albuquerque, NM. Of the primary components, the falling particle receiver, and particle-to-sCO_2 heat exchanger have been demonstrated at the 250 kW$_t$ capacity. The storage component is now being demonstrated as part of the G3P3-USA and G3P3-KSA pilot plants. Storage bin liner materials have been demonstrated by KSU in 2016 and 2019. A flowing particle storage container was demonstrated in 2020 by KSU. The testing presented in this work will be the first to test the particle to wall interactions with monolithic refractory insulation, and to validate a transient thermal transport model with the unique kinetics of bulk solids in funnel-flow where cooler particles near the walls flow inward toward a hot central flow channel. This work will also de-risk and characterize the specific design of the G3P3-USA storage bin.

Keywords: Concentrating Solar Power, Thermal Energy Storage, Flowing Particles

1. Introduction

Concentrating Solar Power (CSP) systems can serve an important role in the overall solar energy strategy because they offer large capacity, long term storage and directly provide heat without electrical conversion. Flowing sand-like particles are being pursued as a media to store and transfer thermal energy because they are well suited to be heated with concentrated sunlight for power production and process heating over diurnal and seasonal cycles. Particles may offer some key advantages over molten salts in that they have been shown to survive temperatures over 1000° C [1] without sintering and may avoid issues with corrosion that have affected solar components and storage bins in particular.

Building on the success of the component-level testing at a capacity of 100 kW$_t$, [2], the Generation 3 Particle Pilot Plant (G3P3) will scale up the test to the 1 MW$_t$ scale (USA) and 2.6 MW$_t$ scale (Saudi Arabia) and add thermal energy storage (TES). In preparation for adding the storage component, modeling and experimentation have been performed by Sandia National Laboratories (SNL), and KSA. This work specifically aims to de-risk the G3P3 storage bin designs and validate a TES model that was developed by The University of

Texas at Austin, which captures the transient and spatial behavior of the bin both in the particle domain and the bin material for flat-bottomed flowing particle storage bins.

2. Modeling

The UT Austin TES model was originally developed to fulfil the need to 1) better understand the transient characteristics of the hot particle storage bin in the G3P3 system, 2) to provide a robust and modular framework that makes the model usable for the investigation and the design of TES systems at scale as well as readily deployable for operation and control applications, and 3) provide a model that can be integrated into a system-level model to allow for general investigation of system performance. The model was first introduced in 2020 [3], where the model's ability to capture the transient characteristics of both funnel flow and mass flow bins through a single discharge process was demonstrated. In 2021 the coupled charge-hold-discharge functionality of the model and a rudimentary system-level model integration were discussed [4].

2.1 Test Objectives

The objectives of the small-scale thermal energy storage bin test campaign are:

1. Validate transient thermal models of heat transfer, resistance, capacitance, and transient outlet temperatures during discharge over consecutive charge/hold/discharge cycles
2. Detect the presence of mechanical stress due to thermal expansion, thermal gradients, ratcheting, and crack propagation and de-risk future bin iterations and larger scales
3. Validate instrumentation methodology and quantify margins and uncertainty in measured data to optimize the information-to-cost ratio for sensor integration in future bin iterations

A single-sample uncertainty analysis will be performed using test-to-test repeatability measurements and strategic perturbations in the test apparatus inputs (inlet temperature, T_0, inlet mass flow rate, $\dot{m}_{in}$, and outlet mass flow rate, $\dot{m}_{out}$). First, the nominal transient temperature profile will be calculated with repeated measurements at each location with a nominal inlet temperature, inlet mass flow rate, and outlet mass flow rate. Next, the inlet temperature and mass flow rates will be perturbed individually and the propagation of these perturbations will be measured in the outlet temperature profiles. A factorial test sequence will be used to characterize the main effects and two-factor interactions of inlet temperature and the mass flow in and out of the bin.

In addition to thermal performance, the sustainability and reliability of the test vessel will be assessed. The interior surfaces will be inspected for crack initiation and propagation and signs of erosion. Temperature gradients on the concrete slab will be measured for heat transfer model validation and stress field modeling development. Strain measurements will be taken at the outer shell to detect ratcheting.

2.2 Test Apparatus

The test stand resides on the side of an existing 1 MW falling particle receiver and can function on or off sun. In the off-sun mode used in this test, an electric furnace is placed on a platform above the test bin with a capacity for three consecutive tests (750 kg) (Figure 1). The particles

are heated to <900° C and a slide-gate is used to control the flow rate of particles into the test bin currently sized for 250 kg of particles. Off-sun testing is beneficial in this test for controlling input temperatures to an uncertainty of ±10° C and for maintaining controlled ambient conditions indoors. The storage bin is 1:8 size scale (1:500 mass scale) of the G3P3 storage bin. The walls are lined with microporous, calcium cilicate, and Tuffcrete 47 (47% Al_2O_3, 47% SiO_2) layers. The roof is comprised of silica fiber modules. Steel shotcrete anchors are placed within the walls. The bin is placed on a refractory concrete slab that is suspended on load cells.

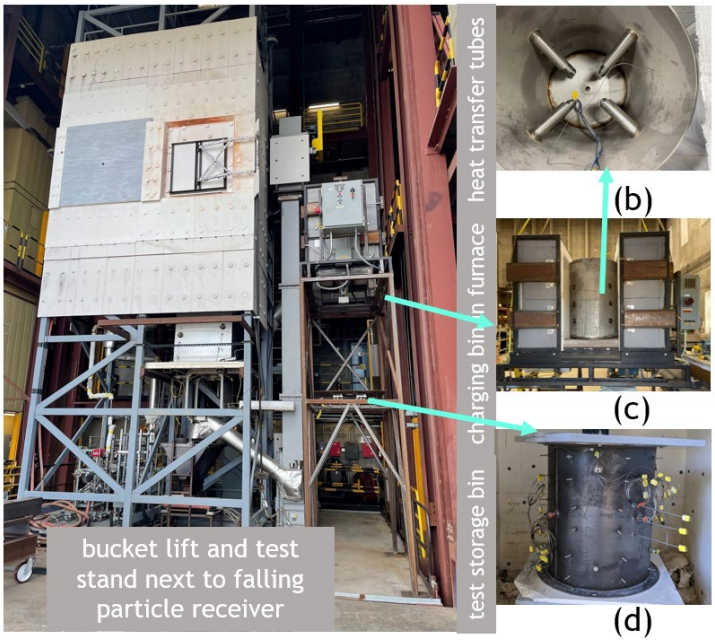

(a)

Figure 1. (a) Test stand mounted next to the falling particle receiver module. (b) charging bin with heat transfer tubes, (c) electric furnace with charging bin, (d) instrumented test bin.

2.3 Geometric and Dynamic Scaling

The bin was scaled geometrically with the characteristic length (*H*) (being 1:8 of the G3P3 6MWh storage bin (0.85 m). The diameter was also scaled 1:8 (0.7 m). TES scaling parameters can be identified in our models or using the Buckingham Pi Theorem:

$$T(Fo,\ \bar{z},\ \bar{r}) = f(Re,\ Pr,\ Bi) \tag{1}$$

where $Fo = \frac{t\alpha}{H^2}$ is the Fourier number, t is time in seconds, α is the thermal diffusivity in $m^2 s^{-1}$ and H is the bin height in meters. $\bar{z}$ and $\bar{r}$ are the nondimensional terms for height and radial distance, $\frac{z}{H}$ and $\frac{r}{H}$, respectively. The Reynolds number characterizes momentum transfer and advection during discharge, the Prandtl number characterizes advection and diffusion of heat inside of the bin, and the Biot number characterizes the relative conduction and convection resistances in the insulation layers. Matching the non-dimensional parameters that govern the TES dynamics is hypothesized to facilitate extrapolation of these test results to the G3P3 scale.

Two inherent scaling challenges are that the diameter and bulk material and thermal properties of the particles cannot be scaled, and available thicknesses for commercially available insulation limit the accuracy of insulation layer scaling. Thus, it is difficult to scale conduction and convective losses. As a solution, , the testing apparatus will first be used to validate the model around the test bin geometry and operating conditions. Following this, the validated model will be used to select the hot storage hold time to make up for differences in heat loss coming from incomplete scaling effects.

2.4 Instrumentation

The instrumentation is designed to validate the model's ability to characterize key measurement points in the bin's thermal profile. The thermal profile is broken down into three hypotheses that capture particle temperatures at the key regions of interests: walls, bulk interior, and outlet.

Wall temperatures

The thermal resistance and capacitance through the wall is described by the composite wall model constructed as a connection of thermal resistors and capacitors of hypothesized time constants as described in Plewe et al 2021 [4]. The wall temperature measurements will test the validity of this lumped 1D model approximation in comparison to a 2D spatially resolved model for the wall insulation layers.

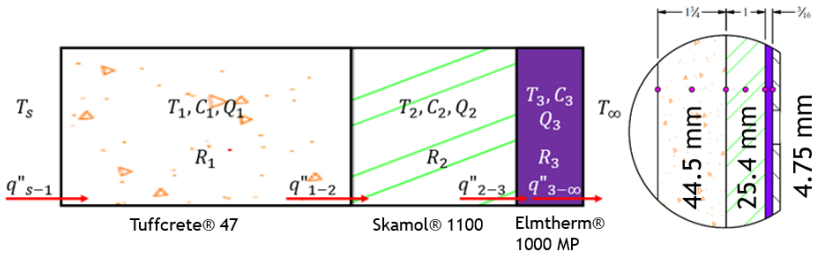

(a) (b)

Figure 2. (a) Thermal resistance/capacitance diagram. (b) Thermocouple placement within walls (dots).

Thermocouples were placed on the surface interface and near the middle of each material layer where T_s is the hot face surface, layer 1 is the cast Tuffcrete 47®, layer 2 is Skamol Super-1100 E®, and layer 3 is Elmtherm 1000 MP® and T_∞ is the ambient air temperature as shown in **Figure 3**. The pattern of 6 thermocouples will be placed in the center of the cylindrical region repeated once at 180° .

(a) (b) (c)

(d) (e) (f)

Figure 3. Process of passing thermocouples through each layer of insulation. (a) Inner shell: To reduce error from conductive effects through the thermocouple, the tips are routed along the perimeter at each layer away from the feedthrough. (b) Microporous layer (c) Calcium

Silicate layer (d) Shotcrete anchors (e) High-density refractory layer (f) Finished interior after bakeout

Particle domain

The particle temperatures throughout the bin are described by the semi-analytic heat kernel model for 5 partial domains shown in Figure 4: 1, Particle-to-wall; 2, Particle-to-floor; 3, Particle-to-air; 4, Flow channel-to-stationary region and 5, Flowing top surface-to-stationary region.

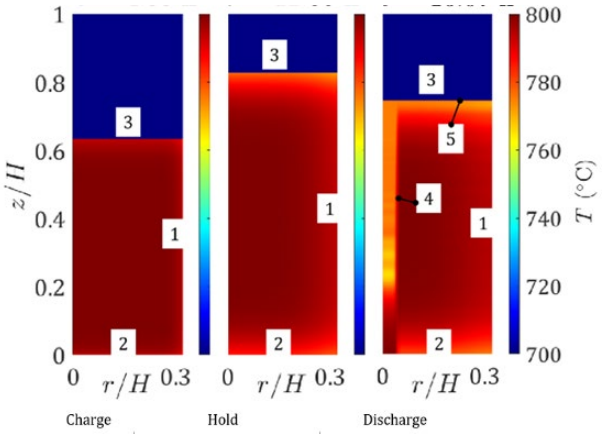

Figure 4. Partial domains for the particle region over three operational phases. Funnel flow discharge presents two additional domains. Figure and nomenclature first described in Plewe et al 2021 [4]

1. The temperature roll-off near the walls is of key interest. There are 6 mm diameter thermocouples protruding into the bin at 25 mm from the wall and a 1.6 mm thermocouple embedded at the junction of the particle bed and interior surface. Additional thermocouples can be routed into the particle bed through the lid as necessary to characterize the rolloff. This is repeated at four locations: two heights and on two sides of the bin.

2. To capture the thermal gradients throughout the stagnant region, thermocouples will be mounted at the bottom corners at the particle-to-wall interface and the outer shell. There will also be thermocouples mounted at the slab-to-particle surface. This is repeated at two locations on opposite sides of the bin. Thermocouples are also mounted inside the slab supporting the test bin and particles (Figure 5).

Figure 5. Thermocouples embedded in heat-resistant concrete slab

3. Radiative effects will be measured by thermocouples located in the hot air pocket in the upper region of the bin and thermocouples will be embedded in the upper lid at the exposed surface, in the middle of the silica fiber insulation, and at the insulation to steel interface.

4. Thermocouples will be mounted in an array through the central axis of the bin. A string will be used to mount the thermocouples with minimal effect on the particle flow.

Outlet temperatures

The boundary coupling methods using direct transposition for the charging and holding phases and Green's function formulae for the discharging phase as described in Plewe 2021 [4] capture particle temperatures at the outlet of the storage bin over the three operational phases. Figure 6 shows the nominal particle temperature at the outlet over the coupled charge-hold-discharge cycle with 2σ bounds on the deviations resulting from the test temperature and mass flow perturbations.

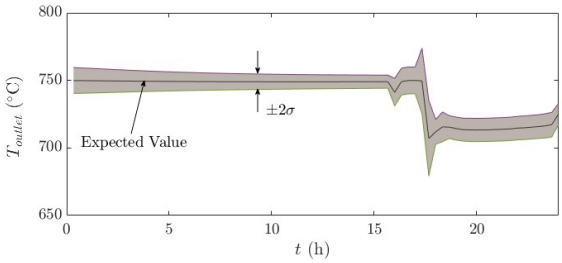

Figure 6. Anticipated experimental results for the thermal storage bin outlet temperature over a single charge-hold-discharge cycle after scaling to the 1MW G3P3 prototype system.

The outlet temperatures will be measured by placing three thermocouples at the center of the outlet hole in the sloped riser. In addition, there will be a single thermocouple placed at the edge of the outlet hole and halfway between the two as shown in Figure 7b. Prior CFD modeling predicted there would be strong gradients across the surface of the outlet [5]. The outlet riser is intended to increase the thickness of the stagnant particle region (Figure 7a) to facilitate a cooler and more evenly heated slab. It is sloped to give an upward vector for the particles during thermal contraction to alleviate ratcheting. The steel plate on top is sized to carry the weight of the particles to bridge over the outlet pipe insulation.

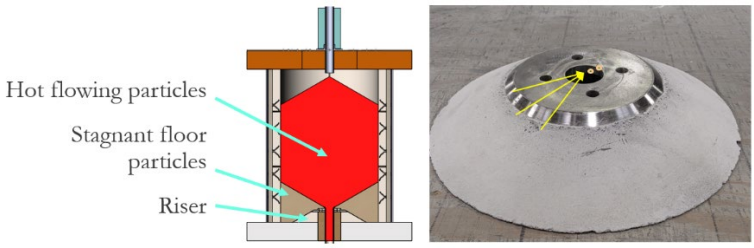

(a) (b)

Figure 7. (a) CAD model cutaway view showing he location of the outlet riser relative to the flowing and stagnant particles. (b) The constructed outlet riser with the outlet measurement locations.

2.5 Test Procedure

The first series of tests were conducted at Allied Mineral Products, LLC, where the test bin was constructed (Table 1). The interior of the bin was heated by a gas burner. A final thermal shock test was performed to determine whether hot particles could be dropped into the test bin if it was not preheated beyond 150° C.

Table 1. Bakeout, thermal cycling, and thermal shock test sequences performed at construction without particles

Standard Bakeout		Thermal Cycling		Thermal Shock	
Temperature (°C)	Hold Time (hr)	Range (°C)	Rate (°C/hr)	Range (°C)	Rate (°C/hr)
100	3	20-800	40	32-145	185
150	3	800	Hold 1 Hour	145-800	185
300	3	800-20	200	800	Hold 1 Hour
425	3	Repeat 5 Times		800-150	-230

Once the test bin arrives at the NSTTF, it will be filled with particles heated to 20, 225, and 550° C to ensure there are no unforeseen issues with particle-to-bin interactions. Then the nominal case will be tested three times. Next, the factorial will be performed controlling for mass flow in, mass flow out, and inlet temperature. The bin will be set upon a scale (Figure 8a) and slide gates (Figure 8b) above and below the bin will be used to control mass flow and inlet temperatures will be set by the electric furnace. The accuracy of the furnace and mass flow will be assessed during commissioning.

(a) (b)

Figure 8. (a) load cells under test bin platform. (b) slide gate and actuator under furnace

3. Preliminary Results

Figure 9a shows readings from the three surfaces: bin interior, the interfacing surface of the Calcium Silicate (Skamol) and hot face layer (Tuffcrete), and the internal surface of the steel shell. Figure 9b shows the interior temperature ramp for the thermal shock test. Ramp rates of 185 °C/hr were achievable. Ramp rates in the G3P3 storage bin of 160-200 °C/hr are possible.

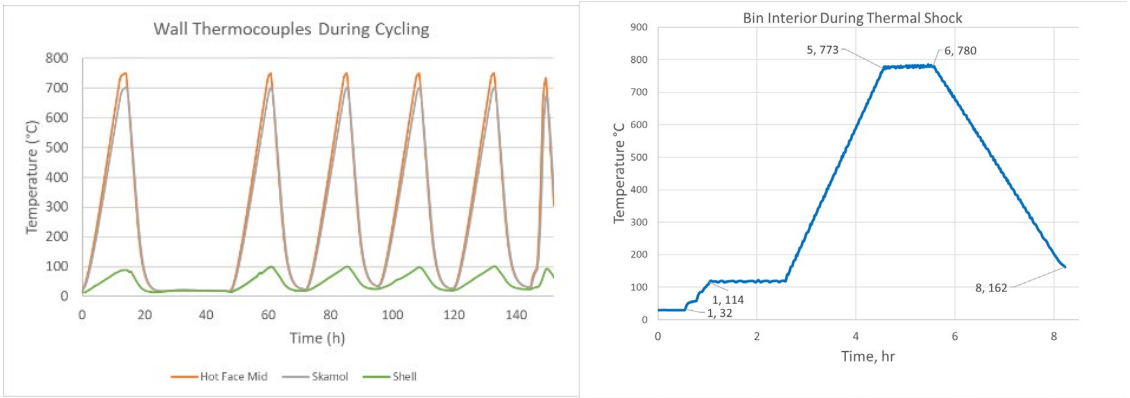

(a) (b)

Figure 9. Thermocouple readings during thermal cycling (a) and thermal shock (b) test

Figure 10 shows the condition of the bin after all air-heated tests. Image (a) shows the effect of bakeout on the expansion joints. The Tuffcrete surface expanded, compressing the ceramic fiber paper (Al_2O_3/SiO_2) and retracted during permanent linear change. The remaining gaps are to be inspected frequently during the particle test series to better understand the dynamics of proppants into small crevices. Image (b) shows the thermocouple embedded at the particle to wall interface circled in red and a thermocouple extended into the bin. The thermal expansion mismatch of the thermocouple and the wall do not cause a gap when the thermocouple breaches normal to the surface, but small flaking does occur when the thermocouple is run parallel to the surface. Figure 10c shows the top surface of the bin after the thermal testing. The layers of the steel shell, Elmtherm, Skamol, and Tuffcrete are presented left to right. The Tuffcrete is bonded to the Skamol. The Elmtherm has experienced permanent deformation and a small air gap remains between the Skamol and the steel shell.

(a) (b) (c)

Figure 10. Final condition of bin interior after air-heated test series. (a) gaps appear around the expansion joint paper (b) minor flaking around embedded surfae thermocouple (c) top surface of test bin

4. Discussion

Future work will compare the measured thermocouples at all locations to the model. Testing with hot particles is planned for late 2022. The key takeaways from the bin cycling tests give insight into how the that the hot face surface performed. As expected, the joint paper is compressed and leaves a residual gap in the joint that is large enough for particle penetration. There are also areas where the paper extends beyond the face of the refractory surface. Part of the value proposition for monolithic refractory construction is that a hermetic metallic liner is not necessary and that standard practices for applying shotcrete with paper joints can be employed without labor intensive finishing procedures. The portions of the paper that extend beyond the wall are vulnerable to erosion, but the G3P3 design induces funnel flow to eliminate vertical motion at the walls. These extended edges will be carefully measured for any changes that could indicate particle contamination.

The permanent deformation of the microporous layer shown in Figure 10c indicates the compression to be expected in G3P3 where microporous insulation doubles as an expansion joint. The change in dimensions will be entered into a model to estimate the final density/conductivity of the microporous layer. Air gaps may have a beneficial effect that potentially offsets some of the increases in conductivity.

5. Data availability statement

The data for this test is unavailable.

6. Underlying and related material

Not applicable.

7. Author contributions

Jeremy Sment: Writing – Original Draft, Formal Analysis, Conceptualization, Methodology, Project Administration, Investigation; Kaden Plewe: Formal Analysis, Methodology, Writing – review and editing; Nathan Schroeder: Formal Analysis, Methodology; Matthew Lambert – Testing, Resources; Dongmei Chen: Supervision, Funding acquisition; Clifford Ho: Supervision, Funding acquisition, Methodology

8. Competing interests

The authors declare no competing interests.

9. Funding

10. This work is funded in part or whole by the U.S. Department of Energy Solar Energy Technologies Office under Award Numbers 34211 and 38711. DOE Project Managers: Matt Bauer, Vijay Rajgopal, and Shane Powers

Acknowledgement

11. Sandia National Laboratories is a multimission laboratory managed and operated by National Technology & Engineering Solutions of Sandia, LLC, a wholly owned subsidiary of Honeywell International Inc., for the U.S. Department of Energy's National Nuclear Security Administration under contract DE-NA0003525. SAND2022-13880 C. The presenter would like to thank the NSTTF technologists: Daniel Ray, Roger Buck, Lam Banh, Kevin Good, and Robert Crandell for building the test stand and Luis Garcia-Maldonado, Aaron Overacker and Madeline Finale for their assistance in configuring the SCADA system.

References

1. R. Knott, et al., *Sintering of Solid Particulates under Elevated Temperature and Pressure in Large Storage Bins for Thermal Energy Storage*, in *Proceedings of the ASME 2014 8th International Conference on Energy Sustainability*. 2014: Boston, MA.
2. M. Carlson, et al., *High-Temperature Particle Heat Exchanger for sCO2 Power Cycles (Award 30342)*. 2020: United States. p. Medium: ED; Size: 180 p.
3. K. Plewe, Jeremy N. Sment, Mario J. Martinez, Clifford K. Ho, Dongmei Chen, *Transient Thermal Performance of High-Temperature Particle Storage Bins* in *SolarPACES 2020*. 2020: Online.
4. K. Plewe, et al. *Transient System Analysis of a Gen3 Particle-Based CSP Plant with Spatially Resolved Thermal Storage Charging and Discharging*. in *SolarPACES 2021*. 2021. Virtual.
5. J. N. Sment, et al. *Testing and Simulations of Spatial and Temporal Temperature Variations in a Particle-Based Thermal Energy Storage Bin*. in *ASME 2020 14th International Conference on Energy Sustainability*. 2020. Denver, CO: ASME.